1994ApJ...434..614G

THE ASTROPHYSICAL JOURNAL, 434:614–626, 1994 October 20
© 1994. The American Astronomical Society. All rights reserved. Printed in U.S.A.

FURTHER MID-INFRARED STUDY OF THE ρ OPHIUCHI CLOUD YOUNG STELLAR POPULATION: LUMINOSITIES AND MASSES OF PRE–MAIN-SEQUENCE STARS

THOMAS P. GREENE[1,2]
Institute for Astronomy, University of Hawaii, 2680 Woodlawn Drive, Honolulu, HI 96822;
greene@ifa.hawaii.edu

BRUCE A. WILKING[1,2,3]
Department of Physics and Astronomy, University of Missouri—St. Louis, 8001 Natural Bridge Road, St. Louis, MO 63121;
C1796@slvaxa.umsl.edu

PHILIPPE ANDRÉ[1]
Service d'Astrophysique, Centre d'Etudes de Saclay, F-91191 Gif-sur-Yvette Cedex, France;
andre@sapvxg.saclay.cea.fr

ERICK T. YOUNG[1,2,3]
Steward Observatory, University of Arizona, Tucson, AZ 85721;
erick@sparky.as.arizona.edu

AND

CHARLES J. LADA[1]
Harvard-Smithsonian Center for Astrophysics, 60 Garden Street, Cambridge, MA 02138;
clada@cfa.harvard.edu

Received 1994 February 7; accepted 1994 April 4

ABSTRACT

We present a new mid-infrared photometric study of the ρ Oph young stellar poplation which includes data for 56 objects. The sources for this study were largely selected from a $K < 10$ mag limited sample in order to reduce the bias of the previous *IRAS*-selected survey of the cloud. This sample was supplemented with fainter sources that are very red as well as sources that also have radio-continuum emission. The $K < 10$ sources are found to have spectral energy distributions predominantly similar to those of reddened T Tauri stars (Class II), while the other sources are mostly either embedded (Class I) or else have little or no circumstellar material (Class III). We develop an empirical technique for estimating the bolometric luminosities of Class II sources from their near-IR data and use it to estimate the luminosities of our newly-observed Class II young stellar objects (YSOs). Most of the newly identified Class II sources have $L \approx 1\ L_\odot$, and several low-luminosity Class I sources are also found. The suspected luminosity segregation between spectral energy distribution classes is reinforced; we find an excess of Class I sources at intermediate ($\sim 10\ L_\odot$) luminosities. Comparisons with Taurus-Auriga YSOs suggest that these high Class I luminosities may be entirely attributable to a higher mass accretion rate in the ρ Oph cloud. We estimate an embedded YSO phase lifetime of approximately $(2 \pm 1) \times 10^5$ yr, which is comparable to that of the Taurus-Auriga clouds. We estimate the masses of the Class II and III cloud population by comparing source luminosities to pre–main-sequence stellar models and find the mean Class II mass to be 1.0 $M_\odot$.

Subject headings: fundamental parameters — infrared: stars — open clusters and associations: individual (ρ Ophiuchi) — stars: pre–main-sequence

1. INTRODUCTION

Mid-infrared studies have played an important role in understanding the early evolution of young stellar objects (YSOs). Not only is much of a YSO's luminosity transferred into the 5–20 μm spectral region by circumstellar dust, but the wavelength dependence of this emission holds important clues to the YSO's evolutionary state. Spectral energy distributions (SEDs) of YSOs have been classified by their slopes from near- to mid-IR wavelengths (e.g., Lada 1987), and their shapes have been successfully modeled, forming a quasi-continuous evolutionary sequence (Adams, Lada, & Shu 1987, hereafter ALS; Myers et al. 1987; Kenyon, Calvet, & Hartmann 1993a; Kenyon et al. 1993b; Calvet et al. 1994). The youngest IR objects are in an embedded evolutionary phase and are characterized by rising mid-IR SEDs (Class I) produced by warm circumstellar dust shells. Class II SEDs are characterized by a peak at near-IR wavelengths followed by decrease in flux through the mid-IR which is much more gradual than expected from a stellar photosphere. Observed Class II SEDs agree well with model predictions of pre–main-sequence (PMS) stars with circumstellar disks (Lynden-Bell & Pringle 1974; ALS) and are typical of Classical T Tauri stars (CTTSs). SEDs of Class III YSOs decrease sharply in luminosity toward longer wavelengths, having little or no IR excess. Class III YSOs are either weak-emission T Tauri stars (WTTs) or young stars near the main sequence with little circumstellar material, and X-ray studies have proved very useful in identifying them. Millimeter-continuum observations further support this evolutionary

[1] Visiting Astronomer at the Infrared Telescope Facility which is operated by the University of Hawaii under contract to the National Aeronautics and Space Administration.

[2] Visiting Astronomer, Multiple Mirror Telescope, operated by the Smithsonian Astrophysical Observatory and the University of Arizona.

[3] Visiting Astronomer, Cerro Tololo Inter-American Observatory, NOAO, operated by the Association of Universities for Research in Astronomy, Inc., under cooperative agreement with the National Science Foundation.

© American Astronomical Society • Provided by the NASA Astrophysics Data System

1994ApJ...434..614G

sequence by determining that circumstellar mass decreases roughly by a factor of 5–10 from one SED class to the next (André & Montmerle 1994, hereafter AM). The PMS interpretation of Class II YSOs is further supported by millimeter-continuum observations, which show that both Class II YSOs and CTTS are point sources with similar fluxes (AM).

Because the *IRAS* survey completely sampled large areas of star formation, mid-IR data from this survey have been the cornerstone for several multiwavelength studies of YSO populations in nearby molecular clouds such as Chamaeleon, Taurus-Auriga, Corona Australis, and Ophiuchus (e.g., Prusti, Whittet, & Wesselius 1992; Gauvin & Strom 1992; Kenyon et al. 1990; Wilking et al. 1992; Wilking, Lada, & Young 1989, hereafter WLY). In the ρ Oph dark cloud (L1688), co-added survey data and higher resolution pointed observations (Young et al. 1985) were combined with near-IR data to construct SEDs and estimate bolometric luminosities for over 50 YSOs (Young, Lada, & Wilking 1986; WLY). From this collection of data, the shapes of the 1–100 μm SEDs were found to form a continuous sequence from Class I to II and rough estimates were made for the lifetime of the Class I phase, the mass accretion rate, and duration of star formation in the cloud. Luminosities appeared to be segregated by SED class with Class I sources dominating at higher luminosities. This suggests that YSOs undergo luminosity evolution as they pass from the Class I to Class II phase. Despite the advances made by these studies, they were limited in several ways. First, the use of *IRAS* data biased these studies against the detection of Class II and III YSOs. Furthermore, the low resolution of *IRAS* has complicated associations of these sources with X-ray near-IR, and radio counterparts and has led to limited sensitivity in crowded regions due to source confusion.

Using ground-based mid-IR observations, we can extend the work of WLY in the ρ Oph cloud with higher resolution than *IRAS* ($\lesssim 8''$ vs. $\gtrsim 45''$) and higher sensitivity. For example, a typical detection limit at $\lambda = 10$ μm on a 3 m class IR telescope is 0.025 Jy ($N = 8$ mag in ~ 600 s) compared to the *IRAS* co-added survey sensitivity of 0.15 Jy in regions of low source density. This improved sensitivity is critical for sampling YSOs throughout the entire depth of the core of Ophiuchus since the large gas column densities correspond to 10 μm extinctions of 2.6–5.2 mag ($A_v = 50$–100 mag; Wilking & Lada 1983; hereafter). These new observations can be guided by recent near-IR camera surveys which have completely sampled large areas of the ρ Oph cloud (Barsony et al. 1989; Greene & Young 1992, hereafter GY; Comeron et al. 1993, hereafter CRBR), thus removing the bias of previous studies toward Class I sources. This will permit a clearer picture of the true numbers and luminosities of Class I versus Class II sources and allow us to explore how this ratio varies between ρ Oph and other clouds.

A potential hazard of a ground-based mid-IR study in a high-extinction cloud core such as ρ Oph is the underestimation of luminosities, particularly those of heavily extincted Class II and III YSOs. Significant fractions of these YSO luminosities will be absorbed by dust beyond circumstellar environments and will not be recovered by ground-based IR observations. Therefore, new techniques must be developed to deredden the photospheres of these PMS stars and estimate their luminosities. For example, CRBR have estimated the luminosities of Class II and III objects in ρ Oph by comparing their near- and mid-IR fluxes to predictions of PMS stellar models at a particular age. A significant advantage of this technique is that the stellar mass immediately follows from the luminosity estimate, and the mass function of these stars can be determined (CRBR). An expanded mid-IR data set and newer PMS models will allow for considerable refinement of such techniques.

We have selected $K < 10$ sources from a recent near-IR survey of the ρ Oph cloud (GY) for a new mid-IR photometric study. Since this selection criterion favors the inclusion of Class II objects, we supplemented this sample with fainter sources which are heavily reddened or associated with radio continuum emission. We further describe this sample and present near- and mid-IR photometric data for 56 of these sources in § 2. In § 3 we present spectral indices and develop new techniques for determining accurate YSO luminosities from these data. Finally in § 4, we discuss the entire YSO population, make comparisons with Taurus-Auriga, and use stellar models to estimate the masses of these YSOs.

2. OBSERVATIONS

2.1. *Sample Selection*

We selected all $K < 10$ sources from GY near the $A_v > 50$ core of the ρ Oph cloud for this new mid-IR study. This selection criterion should not suffer from the Class I selection bias of the WLY *IRAS* study, since a Class II source has more flux in the K band than does Class I source of equal luminosity. For example, the Class I object WL 6 and the Class II object SR 9 both have $L \simeq 2.5\ L_\odot$ (WLY), but SR 9 is approximately 3 mag brighter than WL 6 in the K band (WLY; Elias 1978; GY). Therefore we also included very red ($H-K > 2$) sources with $10 < K < 12.5$ from the GY survey in order to minimize the bias against Class I YSOs. There are 16 new sources (not identified by WLY) in this category, but we observed only four of them including the radio continuum source GY 253. We also supplemented this sample with several other radio continuum sources (e.g., Andre, Montmerle, & Fiegelson 1987, hereafter AMF; Leous et al. 1991, hereafter LFAM; all $K \gtrsim 10$), Hα emission line objects (Wilking, Schwartz, & Blackwell 1987, hereafter WSB), X-ray sources (Montmerle et al. 1983), and *IRAS* sources without mid-IR ground-based data (WLY) in order to make our new sample more complete to the detection of YSOs of all classes. A few of these supplemental sources lie just outside of the $A_v > 50$ cloud core region but still within the confines of the L1688 dark cloud.

We also present photometric data on seven *IRAS*-selected YSOs in the nearby L1689 and L1709 clouds. Most of these data were acquired in 1986 June at the NASA Infrared Telescope Facility (IRTF) with the procedures and techniques described in WLY. We do not include them in our subsequent analysis of the ρ Oph cloud population.

2.2. *Equipment and Data Reduction*

The new photometric data of our source sample are presented in Table 1. These include data from the facility IR cameras, photometers, and bolometers of the IRTF, Cerro Tololo Inter-American Observatory (CTIO), and Multiple Mirror Telescope (MMT). The facilities used and the dates of observations of each source are also presented in the notes of Table 1. References to published photometry used in our following analysis are also listed in this table. Our new photometry is largely in good agreement with existing data, but we have repeated few previous observations and many sources are likely variable.

© American Astronomical Society • Provided by the NASA Astrophysics Data System

1994ApJ...434..614G

TABLE 1

INFRARED PHOTOMETRY

GY IRS	Other[a]	R.A. (1950)	Decl. (1950)	J	H	K	L	M	N	Q
L1688 Sources:										
	SR 22	16 22 22.7	-24 22 55	10.20	9.19	8.70	7.58	8.72	6.58	
	VSSG 19	16 22 56.8	-24 11 01		9.55	9.13			>6.50	
	GSS 28	16 23 15.8	-24 13 37	11.20	8.80	7.80	6.80	6.79	4.56	
	LFAM 1	16 23 20.3	-24 16 07			13.59	10.65	8.94	7.31	4.56
12	GSS 30#2	16 23 21.0	-24 16 13	14.81	11.72	9.89	8.50	8.42	>8.2	
17	DoAr 25	16 23 21.7	-24 36 33		8.35	7.95		6.60	5.89	
21	LFAM 3	16 23 22.1	-24 17 54	14.59	11.76	10.04	7.80	6.51	5.02	
31	VLA	16 23 23.8	-24 16 39			13.30	10.61	>9.00	>7.70	
45		16 23 28.1	-24 32 00	12.38	10.51	8.32			7.67	
65		16 23 31.1	-24 29 43	13.39	10.82	8.92			8.25	
93	WSB 37	16 23 39.4	-24 33 36	10.99	10.62	9.35	8.40	8.58	7.18	
101	ROC 16	16 23 40.9	-24 19 43	>19.60	16.11	12.56	10.15	>8.60	>7.40	
110	VSSG 2	16 23 41.6	-24 13 49	10.95	9.15	8.10	7.09	6.78	5.09	
	VSS 27	16 23 45.0	-24 05 23	9.51	8.34	7.52	6.80	6.46	5.42	
129	WL 18	16 23 47.1	-24 31 43	13.85	11.40	9.98	8.50	7.66	6.88	
135	VSSG 3	16 23 47.8	-24 13 19	12.36	9.81	8.66	7.70	7.65	>7.30	
150	VSSG 6	16 23 52.6	-24 15 47	14.68	11.39	9.58			>5.00	
153	VSSG 5	16 23 52.8	-24 19 39	13.60	11.71	9.96	8.30	7.95	6.62	
156		16 23 53.7	-24 15 49	15.25	11.84	9.91			>8.80	
167	SR 24S	16 23 56.5	-24 38 55	10.21	8.25	7.14	6.01	5.13	3.19	0.88
168	SR 24N	16 23 56.5	-24 38 48	10.85	8.83	7.73	6.27	5.74	3.53	1.57
197	LFAM 26	16 24 03.5	-24 29 48		>17.90	14.63	11.37		7.45	>3.70
224	IRAS 43	16 24 09.4	-24 34 06		13.22	10.38	7.99	7.05	5.59	3.41
228	IRS 32	16 24 10.2	-24 17 01	14.37	11.50	10.06	9.17	7.90	>6.10	
232		16 24 11.4	-24 34 54		12.84	9.66			8.20	
	WSB 45	16 24 12.3	-24 44 52	10.93	9.95	9.69		>8.8	>5.6	
	WSB 46	16 24 13.0	-24 44 58	10.12	9.05	8.76		8.58	>5.4	
245	CRBR	16 24 16.6	-24 32 34	19.00	15.70	12.21	9.27	8.56	6.68	
246	WL 5	16 24 16.6	-24 22 12		14.41	10.35	7.83	6.81	7.14	
253	VLA	16 24 19.9	-24 36 55	16.86	13.24	10.82	9.02	9.06	>7.70	
256	VLA	16 24 20.3	-24 22 57		15.26	12.84	10.98		7.84	
	VSSG 22	16 24 21.5	-24 11 16	13.10	10.72	9.48	8.39	8.52		
257	CRBR	16 24 22.6	-24 22 48	>19.30	15.17	12.34	11.10		8.00	
262	CRBR	16 24 24.7	-24 32 45	15.92	12.15	9.99	7.97	7.67	7.38	
267	VSSG 25	16 24 25.7	-24 24 37	12.57	10.45	9.14		7.91	6.38	
292	IRAS 18	16 24 31.3	-24 34 35	11.49	9.44	7.82	6.30	5.93	4.31	
295		16 24 33.5	-24 31 54	11.51	10.79	9.68			>8.50	
314		16 24 37.6	-24 32 36	11.07	10.20	8.53		6.45	4.90	
351	VSSG 13	16 24 45.2	-24 16 43	10.54	8.20	7.22		6.79	6.86	
372	VSSG 14	16 24 48.3	-24 19 00	9.39	8.15	7.34		7.28	6.54	
400	SR 10	16 24 54.0	-24 19 39	10.35	9.23	8.48		7.47	5.76	
410	VLA	16 24 56.0	-24 33 22	12.85	11.13	9.86	9.14	>9.30	>7.80	
411		16 24 56.2	-24 31 10	13.06	11.47	9.61	>8.30			
453	VSSG 16	16 25 02.2	-24 19 53	8.50	6.96	6.46		6.13	5.98	
	VSSG 15	16 25 07.8	-24 16 44	9.51	7.80	7.14		6.43	6.36	
	WSB 60	16 25 14.6	-24 30 21			9.45	7.51	7.65	5.21	
	SR 20	16 25 21.8	-24 16 02	9.94	9.31	8.24	7.32	6.63	6.32	
	IRAS 64a	16 26 22.2	-24 07 25	9.81	8.29	7.20	6.14	5.25	5.11	
	ROX s39	16 27 33.8	-24 27 51	9.04	8.26	8.00	7.65	7.56	>7.6	
L1689 and L1709 Sources:										
	1 / ROX 43	16 28 18.2	-24 23 39	7.95	7.21	6.70	5.97	6.20	3.30	1.30
	2	16 28 29.0	-24 18 15	10.25	8.79	7.78	6.38		4.31	>1.5
	3 / ROX 44	16 28 31.6	-24 21 13	9.04	7.94	7.28	6.41		4.70	
	4	16 28 34.3	-23 55 05	16.40	12.15	9.29	6.79	5.56	3.99	1.71
	5	16 28 49.7	-24 49 53	11.73	9.47	7.9	6.43	5.21	3.34	2.22
	6	16 28 58.3	-24 50 20	>17.3	13.31	10.43	7.97	6.10	4.23	0.73
	7	16 29 19.0	-24 24 13	12.27	9.80	8.41	7.10	6.55	4.80	2.30

[a] Source names are derived from references cited in the text except as follows:
DoAr: Dolidze & Arakeylan 1959.
GSS: Grasdalen, Strom, & Strom 1973.
IRAS: WLY, Table 1.
IRS: WLY, Table 2.
ROC: André et al. 1987.
ROX: Montmerle et al. 1983.
SR: Struve & Rudkjøbing 1949.
VLA: detected in the radio-continuum by one of us (P.A.).

© American Astronomical Society • Provided by the NASA Astrophysics Data System

1994ApJ...434..614G

M (4.8 μm) and *N* (10 μm) band observations were conducted during 1991 April 28–30 and 1992 May 15 with the MMT and its facility bolometer, using a 5″ aperture. γ Aql and α Boo were used as primary flux standards, while δ Sco was used as a secondary flux standard. We observed α Hyd for an airmass calibrator during the 1991 April run, with typical values of $\tau_M = 0.40$ mag per airmass and $\tau_N = 0.25$ mag per airmass. Frequent observations of δ Sco were used to correct for sky variations and airmass changes during the 1992 run. A chopper throw of approximately 15″ was used, and a typical on-source integration time was 10 minutes. The uncertainty in absolute flux is typically 15%–20%.

J (1.25 μm), *H* (1.65 μm), *K* (2.2 μm), and *L* (3.4 μm) band data were taken with the 1.5 m CTIO reflector during 1989 July 12–19 with the facility 58 × 62 InSb array imager. The data were acquired and reduced in a manner very similar to that described by Wilking et al. (1992). We estimate uncertainties in the absolute photometric calibration to be ±0.06 mag for *J*, *H*, and *K* and ±0.15 mag for *L* data.

IRTF observations were conducted during 1990 June 20–23, 1990 August 3–6, 1991 May 21–22, 1991, June 18–20, and 1992 June 6–8. *J*, *H*, *K*, and *L*-band data were acquired with ProtoCAM, the IRTF 58 × 62 InSb array camera, while *M*, *N*, and *Q* (20 μm) band data were acquired with the Bolo 1 IRTF

TABLE 1—*Footnote continued*

VSS: Vrba, Strom, & Strom 1976.
L1689 and L1709 sources are also numbered sequentially.
NOTE.—References or facilities (CTIO, MMT, IRTF, *IRAS*) and dates listed for each source:
SR22: *BVRI*—Gordon & Strom 1990; *JHKL*—Rydgren, Strom, & Strom 1976; *MN*—IRTF 1991.
VSSG19: *BVRI*—Gordon & Strom 1990; *HK*—VSSG; *N*—IRTF 1991.
GSS28: *BVRI*—Gordon & Strom 1990; *JHKL*—VSSG; *MN*—MMT 1992.
LFAM 1: *KLMNQ*—IRTF 1992.
GY 12/GSS 30#2 (LFAM 2): *JH*—GY; *KL*—IRTF 1991; *M*—MMT 1991; *N*—IRTF 1991.
GY 17/DoAr 25: *BVRI*—Gordon & Strom 1990; *HK*—CTIO 1989; *MN*—MMT 1991.
GY 21/LFAM 3: *J*—GY; *HKL*—IRTF 1992; *MN*—MMT 1991.
GY 31/VLA: *KLMN*—IRTF 1992.
GY 45: *JHK*—GY; *N*—MMT 1991.
GY 65: *JHK*—GY; *N*—MMT 1991.
GY 93/WSB 37: *JH*–GY; *KLMN*—IRTF 1991.
GY 101/ROC 16: *J*—CRBR; *HKLMN*—IRTF 1992.
GY 110/VSSG 2: *RI*—Chini 1981; *JH*—GY; *KLMN*—IRTF 1991.
VSS 27 (also ROX 16): *BVRI*—Gordon & Strom 1990; *JHKL*—CTIO 1989; *MN*—IRTF 1991.
GY 129/WL 18: *J*—GY; *HKLMN*—IRTF 1991.
GY 135/VSSG 3 (LFAM 18): *I*—Chini 1981; *JHKLMN*—IRTF 1991.
GY 150/VSSG 6: *JHK*—GY; *N*—MMT 1992.
GY 153/VSSG 5: *JHKLMN*—IRTF 1991.
GY 156: *JHK*—GY; *N*—MMT 91.
GY 167/SR 24S: *V*—Cohen & Kuhi 1979; *JHKLMNQ*—IRTF 1990.
Gy 168/SR 24N: *V*—Cohen & Kuhl 1979; *JHKLMNQ*—IRTF 1990.
GY 197/LFAM 26: *H*—CRBR; *KLNQ*—IRTF 1992.
GY 224/IRAS 43: *H*—GY; *KLMNQ*—IRTF 1991.
GY 228/IRS 32: *JHKLM*—WLY; *N*—MMT 1992.
GY 232 (LFAM p5): *HK*—GY; *N*–MMT 1991.
WSB 45 (ROX 20 NW): *BVRI*—Gordon & Strom 1990; *JHKLMN*—IRTF 1990.
WSB 46 (ROX 20SE): *BVRI*—Gordon & Strom 1990; *JHKLMN*—IRTF 1990.
GY 245/CRBR: *JH*—CRBR; *KL*—CTIO 1989; *MN*—MMT 1991.
GY 246/WL 5 (ROC 20): *H*—CTIO 1989; *KLMN*—IRTF 1991.
GY 253/VLA: *JHKLMN*—IRTF 1992.
GY 256/VLA: *HKLN*—IRTF 1992.
VSSG 22 (ROC 21): *JHKLM*—IRTF 1992.
GY 257/CRBR: *JL*—CRBR; *HK*—CTIO 1989; *N*—MMT 1991.
GY 262/CRBR: *J*—GY; *H*—CTIO 1989; *KL*—IRTF 1991; *MN*—MMT 1991.
GY 267/VSSG 25: *I*—Chini 1981; *JHK*—GY; *M*—IRTF 1991; *N*—IRTF 1992.
GY 292/IRAS 18: *J*—GY 92; *HKL*—CTIO 1989; *MN*—MMT 1991.
GY 295: *JHK*—GY; *N*—MMT 1991.
GY 314 (LFAM p8): *JHK*—GY; *MN*—MMT 1991.
GY 351/VSSG 13: *I*—Chini 1981; *JHK*—VSSG; *MN*—MMT 1991.
GY 372/VSSG14 (ROC 31): *BVRI*—Chini 1981; *JHK*—Elias 1978; *MN*—MMT 1992.
GY 400/SR 10: *UBVRI*—Chini 1981; *JHK*—GY; *MN*—IRTF 1991.
GY 410/VLA: *JHK*—GY; *LMN*—IRTF 1992.
GY 411: *JHK*—GY; *N*—MMT 1991.
GY 453/VSSG 16: *BVRI*—Chini 1981; *JHK*—VSSG; *MN*—MMT 1991.
VSSG 15: *BVRI*—Gordon & Strom 1990; *JHK*—VSSG; *MN*—MMT 1992.
WSB 60: *KL*—CTIO 1989; *MN*—MMT 1991.
SR 20; *BVRI*—Gordon & Strom 1990; *J*—Rydgren et al. 1976; *HKL*—CTIO 1989; *MN*—MMT 1991.
IRAS 64a: *JHKL*—CTIO 1989; *MN*—MMT 1991.
ROX s39: *BVRI*—Gordon & Strom 1990; *JHKLMN*—IRTF 1992.
1/ROX 43: *UBVRIJHKL*—Walter et al. 1991; *MNQ*—IRTF 1986; 12 μm, 25 μm–*IRAS*.
2: *JHKLNQ*—IRTF 1986; 12 μm, 25 μm, 60 μm—*IRAS*.
3/ROX 44: *UBVRI*—Bouvier & Appenzeller 1992; *JHKLN*—IRTF 1986; 12 μm, 25 μm—*IRAS*.
4: *JHKLMNQ*—IRTF 1986; 12 μm, 25 μm, 60 μm—*IRAS*.
5: *JHKLMNQ*—IRTF 1990.
6: *JHKLMNQ*—IRTF 1986; 12 μm, 25 μm, 60 μm—*IRAS*.
7: *JHKLMNQ*—IRTF 1986; 12 μm, 25 μm—*IRAS*.

© American Astronomical Society • Provided by the NASA Astrophysics Data System

1994ApJ...434..614G

facility bolometer. ProtoCAM images were acquired at the 0".35 pixel^{-1} plate scale, resulting in a 20" × 22" field of view. These image data were acquired and reduced in a manner very similar to that described by Wilking et al. (1992). Absolute photometric uncertainties are estimated to be ±0.05 mag for all J, H and K ProtoCAM data, and ±0.10 mag for L ProtoCAM data.

Three millimeter (5".5) and 4 mm (7".5) apertures were used in acquiring M, N, and Q photometry with the IRTF bolometer. The star α Boo was used as a primary photometric standard, while δ Sco was used as a secondary standard and airmass calibrator. Typical airmass values of $\tau_M = 0.33$ mag per airmass and $\tau_N = 0.20$ mag per airmass. Each source was observed for approximately 10 minutes of integration time. A chopper throw of 15" was used, and the uncertainty in absolute flux is typically 15% (M and N) or 20% (Q).

3. RESULTS

3.1. *Spectral Energy Distributions and Spectral Indices*

We calculated the 2.2–10 μm spectral indices a for all observed sources in Table 1 from the relation:

$$a = \frac{d \log (\lambda F_\lambda)}{d \log \lambda} \quad (1)$$

(as defined in WLY) in order to quantify the natures of their SEDs. We computed a for each object by least squares fitting all data between 2.2 and 10 μm, and we compared these indices to ones which included 20 μm (Q-band) detections when available (Table 1), spanning the range $-0.8 \leq a \leq 0.9$. The 2.2–20 μm indices show no systematic deviations from the 2.2–10 μm ones, suggesting that our 10 μm (N-band) data are not seriously contaminated by silicate absorption features. Hence all further SED analyses were done using only the 2.2–10 μm indices. Upper limit indices were calculated for sources with only 3 σ upper limit N-band data. Our data (Table 1) allowed us to determine spectral indices for 33 sources and give upper limits for 16 sources in the L1688 cloud, and indices were determined for all 7 sources in the L1689 and L1709 clouds. The L1689 and L1709 sources have $-1 \lesssim a \lesssim 1$ (Table 2), similar to the Class I and II sources found by WLY in the L1688 ρ Oph cloud core. Table 2 lists the 2.2–10 μm spectral indices, a of all sources. Henceforth all analysis was done for L1688 sources only.

We now analyze and classify the distribution of these indices. We classify sources with $a > 0.3$ as Class I, $0.3 > a \geq -0.3$ as "flat spectrum," $-0.3 > a \geq -1.6$ as Class II, and $a < -1.6$ as Class III YSOs. We adopt this revised scheme because recent work has refined the definitions of SED classes to better correspond to physical stages of YSO evolution. AM determined that YSOs with $a \lesssim -1.5$ have significantly less millimeter-continuum flux than more positive index Class II objects, strongly suggesting that there is considerably less circumstellar material surrounding these stars. Greene (1994) finds that YSOs with $a \gtrsim -0.3$ have near-IR spectra which are strongly veiled by continuum emission from hot circumstellar dust, indicative of an intimate relationship between star and environment atypical of PMS T-Tauri type objects. It is therefore likely that YSOs with $-0.3 > a \gtrsim -1.5$ are PMS stars with considerable amounts of circumstellar material that does not veil their photospheres in the near-IR. We note that our sample has no sources with $-1.9 < a < -1.6$ (nor does WLY) or $-0.3 < a < 0$, so there are natural gaps in the distribution near these newly revised

TABLE 2

SPECTRAL INDICES AND LUMINOSITIES

GY IRS	Other[a]	a (2–10 μm)	L_{cal}[b] ($L_\odot$)	L_{est}[c] ($L_\odot$)	δL[d] ($L_\odot$)	A_V[e] (mag)
L1688 Sources:						
197	LFAM 26	1.4	~0			
	LFAM 1	0.9	~0			
245	CRBR	0.4	~0			
21	LFAM 3	0.2	0.3			
256	VLA	0.2	~0			
224	IRAS 43	0.0	0.2			
257	CRBR	-0.1	~0			
168	SR 24N	-0.4	1.3	3.7	1.1	10.6
167	SR 24S	-0.4	2.2	5.9	1.5	10.4
	WSB 60	-0.4	0.2	...	...	...
314		-0.6	0.5	0.2	...	0.7
292	IRAS 18	-0.7	0.8	4.1	1.3	15.0
153	VSSG 5	-0.9	0.1	0.7	0.5	15.3
	GSS 28	-0.9	0.7	5.4	3.3	11.6
129	WL 18	-1.0	0.1	0.7	0.4	15.2
110	VSSG 2	-1.0	0.5	2.3	0.2	9.6
246	WL 5	-1.0	0.2			
267	VSSG 25	-1.1	0.2	1.2	0.0	12.8
400	SR 10	-1.2	0.5	0.9	0.1	3.5
262	CRBR	-1.4	0.1	2.5	0.4	27.7
	VSS 27	-1.5	1.0	2.0	0.0	4.3
	IRAS 64a	-1.5	1.4	3.8	0.2	8.2
93	WSB 37	-1.5	0.2	0.2	...	~0
17	DoAr 25	-1.6	0.8	1.0	...	~0
	SR 20	-1.6	0.6	0.5	...	~0
	SR 22	-1.6	0.4	0.6	0.0	0.9
232		-1.9				
372[f]	VSSG 14	-2.3	1.2			12.4
	VSSG 15	-2.3				
65		-2.4				
45		-2.4				
453	VSSG 16	-2.5				
351	VSSG 13	-2.6				
31	VLA	<0.4	~0			
101	ROC 16	<0.2	~0			
150	VSSG 6	<0.0				
228	IRS 32	<-0.3				
	WSB 45	<-0.4	0.1			
	WSB 46	<-0.8	0.5			
253	VLA	<-1.0	~0			
	VSSG 19	<-1.2				
410	VLA	<-1.6	0.1	0.7	...	14.0
	VSSG 22	<-1.6	0.1	2.6	...	13.4
12	GSS 30#2	<-1.9	0.1	3.1	...	24.9
135	VSSG 3	<-2.0	0.2	7.9	...	16.9
411		<-2.0				
156		<-2.1				
295		<-2.1				
	ROX s39	<-2.5	0.9	2.3	1.3	
L1689 and L1709 Sources:						
	6	0.9	0.6			
	4	0.3	0.8			
	5	0.0	1.3			
	7	-0.6	0.5	3.1	0.7	15.1
	2	-0.7	1.0	2.1	0.1	7.2
	1 / ROX 43	-0.8	3.5	2.8	0.2	~0
	3 / ROX 44	-1.2	1.7	2.3	0.3	2.7

[a] See Table 1 notes for explanations of source names.

[b] Calorimetric luminosity is a lower limit estimate derived from all data listed in Table 1 and cited in its notes; see text.

[c] Luminosity estimate is calculated from empirical relations (eqs. [2] and [3]) for Class II sources and from DM—McCaughrean (1993) PMS models for Class III sources associated with the cloud; see text.

[d] Uncertainty in luminosity estimate is one-half the absolute value of the difference of the luminosities calculated from equations (2) and (3).

[e] Visual extinction in magnitudes to each YSO is derived from RL and the intrinsic source colors discussed in text.

[f] The spectral type of this source (A5–7) indicates that its mass is beyond the applicable range of this stellar model luminosity relation. Visual extinction was calculated from this spectral type.

© American Astronomical Society • Provided by the NASA Astrophysics Data System

1994ApJ...434..614G

SED boundaries. Furthermore, we note that four objects in L1688 have indices $a \approx 0$, not clearly positive or negative (see Table 2). For this reason we classify them as "flat spectrum" sources which have an uncertain evolutionary status. This leaves three Class I objects, 19 Class II objects, and seven Class III objects. Eight of the upper limit spectral index sources are also Class III by these criteria, while the remaining eight are likely either Class II or III. All Class I and flat spectrum sources as well as 10 of the Class II objects are new determinations.

In Figure 1 we plot the SEDs of all sources in Table 2 with $a \geq -1.6$. The long-wavelength slopes of nearly all source SEDs in Figure 1 are well characterized by their spectral indices, a, with the exception of WL 5. Therefore we retain our spectral index classifications of all SEDs except that of WL 5, which is probably a heavily reddened Class III SED.

3.2. *Luminosity Estimates*

Accurate luminosity estimates are imperative for achieving the goals of this study. Therefore we now develop three independent methods of estimating YSO luminosities and apply them to the newly observed sample. These techniques involve calorimetric flux integration, correlation of luminosities with empirical data, and luminosity determination from PMS models.

3.2.1. *Calorimetric Technique*

First, we estimate bolometric source luminosities by applying the calorimetric technique to our data set which we supplemented with shorter wavelength photometry when available (see Table 1, and notes therein). Calorimetric luminosities were calculated by trapezoidal integration of observed flux densities over wavelengths of observation and extrapolation to infinite wavelengths by assuming a spectral index of $a = -1$. Luminosity estimates of Class II and III YSOs are insensitive to the details of this extrapolation since they have little luminosity at wavelengths beyond 10–20 μm. Our limited data ($\lambda \leq 20$ μm) have too little long-wavelength information to determine Class I source luminosities accurately, so we only offer our calorimetric estimates as lower limits to their true luminosities. However, our calorimetric luminosities may closely estimate the bolometric luminosities of Class II objects with the following exceptions. The calorimetric luminosity technique assumes isotropic radiation, and it may yield luminosities that are up to a factor of 2 too high if most of the luminosity is radiated from a face-on disk (WLY). Class II and especially Class III YSOs have considerable flux at short wavelengths, and the calorimetric technique may not recover this luminosity if short-wavelength data is either not available or else heavily reddened by foreground dust. Many Class III objects have uncertain associations with the cloud and may be field stars, but ones with X-ray, radio or Hα emission (ROX, ROC, VLA, LFAM, or WSB sources in Tables 1 and 2) are probably YSOs in the cloud. Hereafter we concentrate on more accurately determining the luminosities of Class II sources, by far the most numerous class in this study.

3.2.2. *Correlation with IR Flux Observations*

The observed near- to far-IR SEDs of Class II sources exhibit a high degree of similarity in their overall shapes (Lada & Wilking 1984, hereafter LW; Rucinski 1985). Stars with Class II SEDs are widely interpreted as obscured PMS T Tauri type stars ($M \leq 2.5\ M_\odot$), evolving along Hayashi tracks in the H-R diagram. These tracks are nearly vertical and closely spaced in effective temperature, so there is little dispersion in intrinsic source colors. This is supported observationally by the small spread in near-IR colors e.g., $J-H$) of both CTTSs and WTTSs in relatively unobscured regions (e.g., Strom, Strom, & Merrill 1993, hereafter SSM). Consequently, a correlation should exist between the bolometric luminosities of Class II sources and their dereddened fluxes at near-IR wavelengths.

The J band is ideal for dereddening since its wavelength is both long enough to allow the detection of Class II objects in moderately obscured clouds, and it is also close to the wavelength of peak flux from PMS stellar photospheres. The J band wavelengths are also too short to include much emission from warm ($T < 2000$ K) circumstellar dust around PMS stars, resulting in a high ratio of photospheric to circumstellar flux. The J band is also less sensitive to opacity effects in late-type stars than the H and K near-IR bands (e.g., see Laçon & Rocca-Volmerange 1992). The relatively narrow effective temperature range of PMS stars (3000–5300 K; D'Antona & Mazzitelli 1994, hereafter DM) ensures that flux in the J band samples approximately the same fraction of stellar luminosity over a considerable range of masses. However, the J band is sensitive to extinction of photospheric flux by either circumstellar (e.g., high-inclination disks) or intervening cloud material. Therefore observed J-band fluxes of Class II YSOs must be dereddened before attempting to correlate them with bolometric luminosities.

In order to examine this suspected correlation, we plotted the bolometric luminosities of Class II YSOs ($-0.3 > a \geq -1.6$) against their dereddened J fluxes. Their calorimetric luminosities were determined from data over a range of at least 1–25 μm, and sometimes as broad as 0.36–100 μm. We restricted this analysis to presumably low-mass sources in the ρ Oph, Taurus-Auriga, Cha I, and R Cr A clouds with well-determined bolometric luminosities and spectral indices. Sources with double-peaked (Class IID) SEDs were excluded. Photometric data and bolometric luminosities from WLY, Ward-Thompson (1993), Kenyon et al. (1990), Rydgren et al. (1984), Rucinski (1985), Prusti et al. (1992), and Wilking et al. (1992) were used to compile a sample of Class II sources with J- and H-band photometric data. Five sources were eliminated because their large reddenings ($J-H > 2.0$) imply that their calorimetric luminosities may be significantly underestimated, leaving 42 sources in this sample. We dereddened J-band fluxes of all sources by assuming intrinsic Class II source colors of $(J-H)_0 = 0.8$ and applying the Rieke & Lebofsky (1985, hereafter RL) reddening law. SSM determined that this $(J-H)_0$ is the average dereddened value for Taurus-Auriga CTTSs.

J-band magnitudes were dereddened with the relation $J_0 = J - 2.64E(J-H)$ (RL). Dereddened J band absolute fluxes, $F(J_0)$, were calculated from these J_0-values and the distance modulus of each cloud. The sources in each cloud exhibited a good linear correlation between $F(J_0)$ and bolometric luminosity, $L_{\rm bol}$, with correlation coefficients from $r = 0.88$ to $r = 0.96$. For the combined sample we find a linear correlation

$$L_{\rm bol}(L_\odot) = (6.61 \pm 0.39) \times 10^9 F(J_0)(\mathrm{W\ m^{-2}\ \mu m^{-1}}) - (0.06 \pm 0.11) \quad (2)$$

with a correlation coefficient $r = 0.94$. Uncertainties in equation (2) are 1 σ. Figure 2 is a linear plot of $F(J_0)$ versus $L_{\rm bol}$ for these sources. The linear fit for these YSOs given by equation (2) is also plotted in Figure 2.

© American Astronomical Society • Provided by the NASA Astrophysics Data System

1994ApJ...434..614G

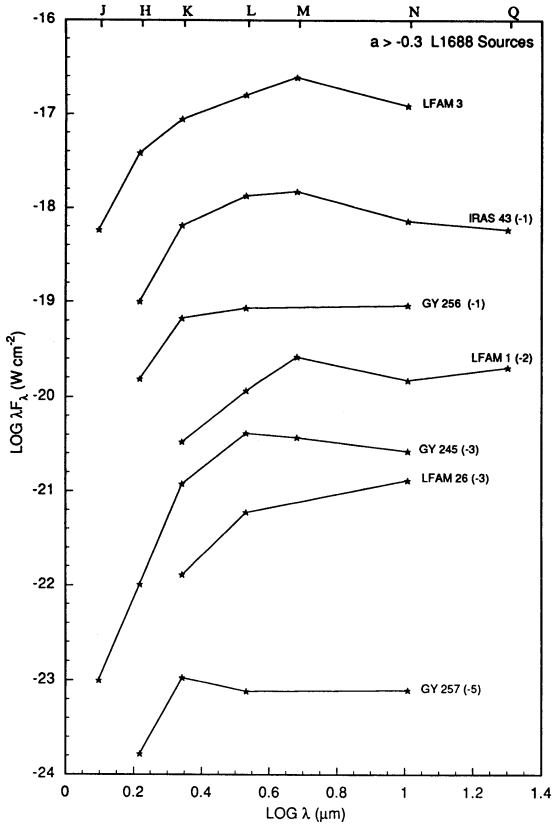

FIG. 1*a*

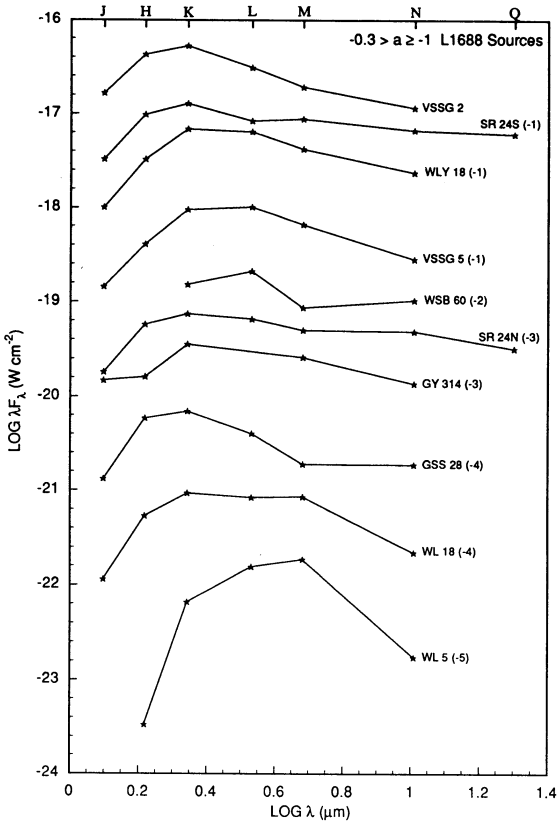

FIG. 1*b*

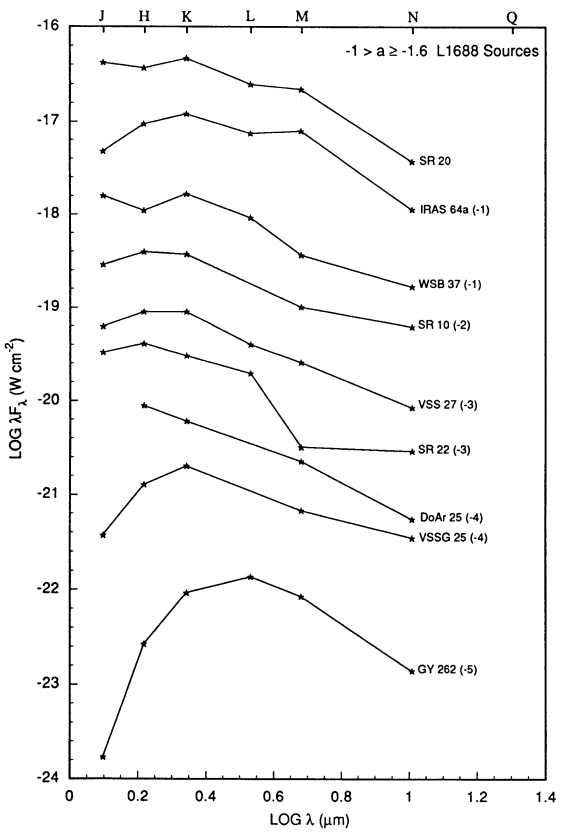

FIG. 1*c*

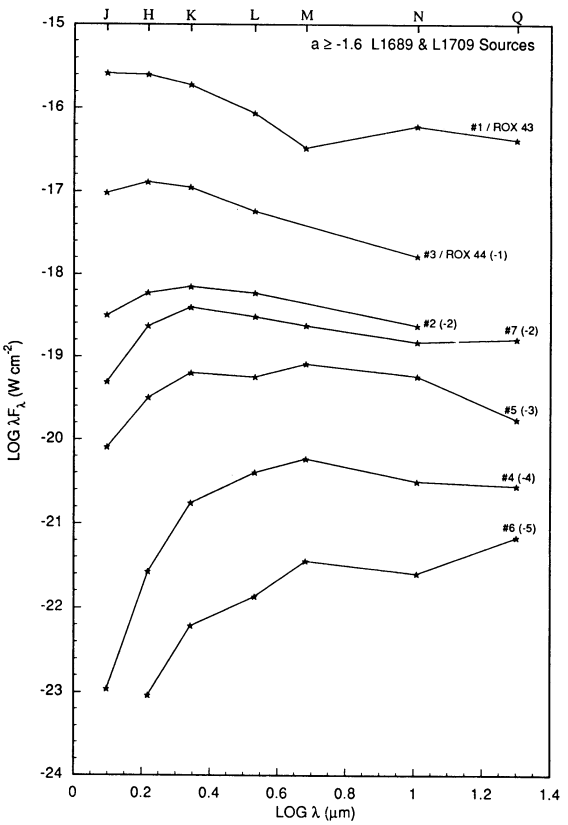

FIG. 1*d*

FIG. 1.—Spectral energy distributions of all sources with $a \geq -1.6$. Panels (*a*)–(*c*) group L1688 cloud sources by spectral index, while (*d*) shows L1689 and L1709 cloud sources. All fluxes were computed from data values in Table 1, and the most common source names are given. The number next to each source name is the power of 10 used to scale the spectral energy distribution.

© American Astronomical Society • Provided by the NASA Astrophysics Data System

1994ApJ...434..614G

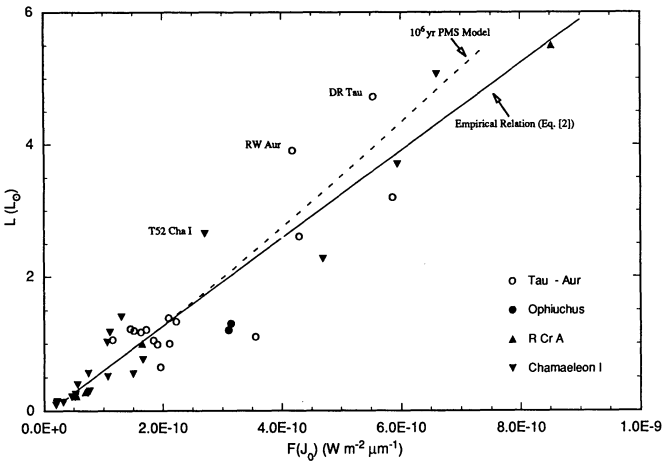

FIG. 2.—Linear L_{bol} vs. $F(J_0)$ plot of Class II YSOs in Taurus-Auriga, Chamaeleon I, R Corona Australis, and ρ Oph clouds with well-determined calorimetric luminosities. The empirical linear fit to the data is shown (*solid line*), along with the DM 10^6 yr PMS model isochrone (*dashed curve*). The marked sources T52 Cha I, RW Tau, and DR Tau have large near-IR excesses and substantial accretion luminosities.

Not all sources in our new data (Table 1) have *J*-band detections due to low fluxes at these wavelengths. Therefore we also examined the correlation of bolometric luminosity and dereddened *K*-band flux for the four-cloud sample of Class II YSOs with *H* and *K* photometric data. We followed a dereddening procedure similar to that of the *J*-band data, limiting the sample to 49 relatively unreddened sources ($H-K < 1.5$; some have no *J* data). SSM show that CTTSs have a wide range of $H-K$ values (0.2–1.2 or more), which indicates that adopting a single mean intrinsic $H-K$ value will not represent these sources well. However, the SSM data show that most CTTSs (without large excesses) have $0.2 < H-K < 0.8$ and can be represented with a single intrinsic $H-K$ value. Therefore we adopted a mean intrinsic $(H-K)_0 = 0.5$, the mean dereddened value of SSM CTTS sources without large near-IR excesses. This mean intrinsic $(H-K)_0$ should apply reasonably well to all sources in our four-cloud Class II sample since none have near-IR excesses greater than $(H-K)/(J-H) = 1.0$.

K-band magnitudes of these sources were dereddened with the relation $K_0 = K - 1.82E(H-K)$ (RL). Dereddened *K*-band absolute fluxes, $F(K_0)$, were calculated from these K_0-values and the distance modulus of each cloud. The sources in each cloud exhibited a good linear correlation between $F(K_0)$ and L_{bol} with correlation coefficients from $r = 0.84$ to $r = 0.93$. For the four-cloud sample we find a linear correlation

$$L_{bol}(L_\odot) = (9.98 \pm 0.58) \times 10^9 F(K_0)(\mathrm{W\ m^{-2}\ \mu m^{-1}}) + (0.26 \pm 0.10) \quad (3)$$

with a correlation coefficient of $r = 0.93$. Uncertainties in equation (3) are 1 σ.

Some of the uncertainties in equations (2) and (3) and scatter in their correlations can be traced to uncertainties in object distances, different epochs of near- and far-IR photometry, age-dependent luminosity effects, and extinction or disk inclination effects on L_{bol}. Nevertheless, the slopes of our empirical relations are statistically uncertain to only ~5% (see eqs. [2] and [3]). *The good overall correlation demonstrates that we can successfully estimate L_{bol} of Class II YSOs from their near-IR photometry without supplemental far-IR data.*

3.2.3. *Determination from PMS Models*

The bolometric luminosities of PMS stars can also be related to their near-IR fluxes via theoretical models. *J*-, *H*-, and *K*-band fluxes were computed for the low-mass PMS CM Alexander models of DM (Canuto & Mazzitelli [1992] convection with Alexander, Augason, & Johnson [1989] and Rogers & Iglesias [1991] opacities). These fluxes were determined by using near-IR data of stellar atmospheres at each effective temperature of the DM models and were kindly provided in advance of publication by M. McCaughrean (1993). These calculations show that the *J*-band fluxes of these PMS models are also proportional to bolometric luminosities. The least-squares linear fit to the 10^6 yr isochrone is $L_{bol}(L_\odot) = (7.4 \pm 0.1) \times 10^9 F(J_0)(\mathrm{W\ m^{-2}\ \mu m^{-1}})$ with a correlation coefficient of 0.997 for $0.10\ M_\odot \leq M \leq 2.5\ M_\odot$. The 3×10^6 yr models have a slightly steeper correlation, $L_{bol}(L_\odot) = (9.0 \pm 0.1) \times 10^9 F(J_0)(\mathrm{W\ m^{-2}\ \mu m^{-1}})$, while the 5×10^5 models have a slightly shallower correlation, $L_{bol}(L_\odot) = (7.2 \pm 0.1) \times 10^9 F(J_0)(\mathrm{W\ m^{-2}\ \mu m^{-1}})$. The 10^6 yr DM-McCaughrean model isochrone is also shown in Figure 2 with the Class II sample data and empirical relation (eq. [2]). Comparison of the data and models is quite instructive because the models are fairly insensitive to age. DM also show that different opacity and convection schemes change the model effective temperatures and luminosities by only about 5% for a 10^6 yr old 1 $M_\odot$ star.

We now proceed to interpret the data in terms of the 10^6 yr (characteristic CTTS age) model shown in Figure 2. First, we note that the slope of this model is approximately 10% steeper than the empirical fit to the data (eq. [2]). This can be understood if the bolometric luminosities of the YSOs are underestimated by about 10% or else the average *J* flux of a Class II YSO is composed of approximately 90% stellar emission and 10% circumstellar emission. Figure 2 also shows that several sources are located above the 10^6 yr PMS model isochrone. Interestingly, the three largest near-IR excess sources in the data set have large fractions of their luminosities above the model curve. T52 Cha I, RW Aur, and DR Tau have near-IR excess values $(H-K)/(J-H) \geq 0.80$, and they all lie significantly above the model curve. This can be understood if these objects have excess luminosities due to mass accretion from circumstellar disks.

3.2.4. *Luminosity Estimates of ρ Oph Sources*

Estimates of bolometric luminosities of sources in our new sample are presented in Table 2. These sources include all Class I, flat spectrum, and Class II sources. We also present luminosity estimates for Class III sources that are known to be associated with the cloud, either by WLY determinations or radio-continuum or X-ray emission. Calorimetric luminosities are given for all of these sources, but we present them as lower limits for Class I, flat spectrum, and Class III sources. All three of the Class I sources are new discoveries and are probably low luminosity, $L \leq 1\ L_\odot$. This is supported by their calorimetric lower limit luminosity estimates as well as by their nondetection in the WLY *IRAS* study which was complete to the detection of $\sim 1\ L_\odot$ Class I YSOs. Extinctions to each source presented in Table 2 are calculated from Table 1 data assuming a RL extinction law and appropriate intrinsic colors (e.g., see § 3.2.2).

We assert that the empirical relations (eqs. [2] and [3]) provide the best estimates of Class II source luminosities given the available data, better than a factor of 2 of true bolometric luminosities (see Fig. 2). Unlike the calorimetric estimates,

© American Astronomical Society • Provided by the NASA Astrophysics Data System

1994ApJ...434..614G

applying these empirical relations recovers bolometric source luminosities well by correcting observed fluxes for interstellar extinction, especially important in the dusty ρ Oph cloud. The Class II sources in our new sample have the same spectral index value range as the sample of objects used to produce these relations, and the PMS models have shown that the L_{bol} versus $F(J_0)$ relation is not very sensitive to age. We calculated the L_{est} values in Table 2 for each Class II source by computing the mean of the luminosity values computed from both equations (2) and (3) after dereddening the requisite J, H, and K data when available. Luminosity estimate uncertainties δL presented in Table 2 are the absolute values of one-half the difference between the J and K empirical luminosity estimates (eqs. [2] and [3]). L_{est} values are generally higher than the calorimetric estimates in Table 2, confirming that they recover more luminosity. L_{est} was calculated only from equation (3) for DoAr 25, and no L_{est} value could be calculated for WSB 60 because of limited near-IR data (Tables 1 and 2). No L_{est} value was calculated for WL 5 because its SED shows that it is probably a Class III source (see § 3.1). L_{est} was calculated from equation (2) only for GY 314, GY 93, and SR 20, large near-IR excess sources [$(H-K)/(J-H) > 1.5$; see § 3.2.2].

Five Class III objects known to be associated with the cloud are also assigned L_{est} values in Table 2. Their L_{est} values were calculated from their dereddened J-band data applied to the 10^6 yr DM-McCaughrean model luminosity relation (see § 3.2.3), adopting the models' mean intrinsic $(J = H)_0 = 0.6$. These models physically represent Class III sources, and they yield luminosities similar to those determined by our empirical relation for Class II YSOs (Fig. 2). The K5 spectral type of ROX s39 (Bouvier & Appenzeller 1992) and the very low calorimetric luminosity estimates of these sources suggest that they are within the mass range of the models. However, Gordon & Strom (1990) show that VSSG 14 (Vrba et al. 1975) is an A5–7 star, so we do not calculate L_{est} for it since its mass is beyond the range of the models. Spectral types for the four remaining Class III SYOs are needed to confirm their low-mass natures.

Examination of our empirical L_{bol} versus $F(K_0)$ relation (eq. [3]) shows that a 1 $L_\odot$ Class II YSO would have an observed K magnitude of 7.9 at the distance of the ρ Oph cloud, verifying that our $K < 10$ sample selection criteria is adequately sensitive to the detection of 1 $L_\odot$ Class II YSOs near the front of the cloud. However, a 1 $L_\odot$ Class II YSO embedded more than halfway into the cloud core would have its K magnitude extincted by more than 2.5 mag (mean $A_v \simeq 50$ mag and $A_k \simeq 0.1A_v$), making it fainter than our $K < 10$ magnitude limit. Therefore the $K < 10$ selection criterion is insensitive to the complete detection of $L = 1\ L_\odot$ Class II YSOs embedded more than halfway into the observed cloud region. However, there are an increasing number of Class II YSOs in this study down to 1 $L_\odot$, so it appears that our new sample is complete to 1 $L_\odot$ over most of the observed region.

4. DISCUSSION

We have combined our new L1688 source sample with the previously studied YSOs in the cloud in order to produce a more accurate description of the population than provided by any individual study to date. The data of WLY and LW were used to recompute the spectral indices between 2.2 μm and 10 μm for all objects in those studies which were not reobserved as part of this work. We also combined the luminosities of the new source sample with those of cloud members listed by WLY which were not reobserved for this study. Recently resolved *IRAS* data (Ward-Thompson 1993) and data from this study were used to better estimate the calorimetric luminosities of 11 WLY sources. L_{est} luminosities were calculated and adopted for five previously studied Class II sources without well-determined luminosities. L_{est} values of Class II and III YSOs in this study (Table 2) were adopted as their bolometric luminosities. Additionally, GY 11 was also included in the combined sample since CRBR present 2.2–10 μm data which show that it is a flat spectrum source. The combined sample contains a total of 80 YSOs, including 71 with determined spectral indices and nine with upper limits. Seventy of the 80 YSOs have luminosity estimates, while 10 do not.

4.1. *Spectral Energy Distributions and Source Classification*

Figure 3 shows the distribution of spectral indices for the combined sample. This figure shows that most sources in this new study are Class II YSOs that have smaller indices than those in the *IRAS*-selected sample studied by WLY. Indeed, inspection of Figure 3 clearly shows that the WLY *IRAS* survey best detected Class I objects, while this mostly K magnitude limited (and radio continuum selected) survey was better at detecting Class II and III YSOs. None of the newly observed $K < 10$ sources are Class I, and we note that all radio continuum sources in our new sample are either Class I or III (see Table 2). Therefore these two complementary surveys when combined yield a less biased picture of the ρ Oph cloud young stellar population. However, this combined sample is still biased against the detection of Class III YSOs, since such stars cannot be positively distinguished from foreground or background field stars without other data (e.g., Hα, X-ray, or radio), and these data have been associated with only a fraction of the cloud's IR sources. Class III YSOs also have less K-band and mid-IR flux than Class II ones of equal mass, so they are expected to be underrepresented in the mostly IR-selected combined sample.

Figure 3 shows that in fact the combined sample has few more Class I YSOs but more Class II objects than found by WLY. Of the 71 sources with determined spectral indices, 16 are Class I, another 16 have flat SEDs, 33 are Class II, and six are Class III. These classifications were determined by spectral index as discussed in § 3.1, with the exception of WL 5 which we classify as a Class III YSO due to its reddened SED (see

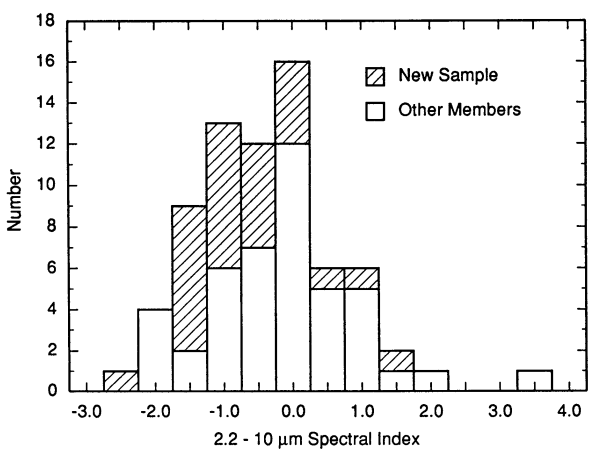

FIG. 3.—The 2.2–10 μm spectral index distribution of the new L1688 sample along with the previously studied population which was not reobserved herein. Upper limit spectral indices are not included.

© American Astronomical Society • Provided by the NASA Astrophysics Data System

1994ApJ...434..614G

§ 3.1), radio, and X-ray emissions (AMF; Montmerle et al. 1983; see Table 1). Another nine sources with spectral index upper limits $a < -1.6$ have been associated with the cloud as Class III sources because of either WLY determinations or additional radio or X-ray data. Additionally, new *ROSAT* results (Casanova et al. 1994) indicate that there may be up to 20 additional $L_{bol} \gtrsim 1\ L_\odot$ X-ray YSOs in the dense cloud core, but to date most of these new YSOs have uncertain IR source associations. This issue may be resolved when more sensitive radio continuum and X-ray data with better positional accuracies become available. It is likely that even more near-IR sources in the cloud core (e.g., up to 40 GY sources with $K > 10$) are YSOs without strong emissions at other wavelengths, but these are difficult to distinguish from foreground or background field stars.

The ρ Oph cloud environment must also be considered when classifying YSOs based on their near-IR spectral indices as done above. Kenyon et al. (1990) and AM have argued that the high extinction of the L1688 core region (mean $A_v \simeq 50$) can be responsible for steepening the SEDs of YSOs deeply embedded in the cloud. Therefore, the combined all-cloud sample described above may actually have more Class II (and III) and fewer Class I YSOs than calculated by our adopted spectral index classification scheme. The 2.2–10 μm spectral indices of YSOs can be increased by as much as 0.5 when extincted by $A_v = 50$ mag (Rieke & Lebofsky 1985 extinction law). In order to estimate the maximum likely magnitude of this effect, we could reclassify the sources in the combined sample after subtracting 0.5 from their near-IR indices, *a*. This reclassification would result in a total of 10 Class I, six flat spectrum, and 41 Class II YSOs. The combined number of flat spectrum and Class I sources would be reduced by half, while the number of Class II YSOs would be increased by 20%. A similar reduction in the number of Class I and flat spectrum sources was also found by AM when they reclassified sources based on individual interpretations of their mid-IR (3.4–20 μm) ground-based SEDs. However, we consider these reclassification results as the most extreme effects possible by reddening within the cloud. Our examination of the source SEDs in this new study (§ 3.1 and Fig. 1) and the *IRAS* data presented in WLY show that fewer than 10% of the sources in the combined sample are likely to have SED classfications different from their non–reddening-corrected near-IR ones (see also Zinnecker, McCaughrean, & Wilking 1993), and we have already reclassified WL 5. Therefore, we retain the results of our non–reddening-corrected spectral index classification for all other YSO SEDs, resulting in the original tally.

4.2. *Luminosity Function of the YSO Population*

The luminosity function of all YSOs is shown in Figure 4 and is grouped by SED classification. Class I and flat spectrum YSOs were grouped together as Class I because recent work suggests that these sources may have intrinsically similar evolutionary states, but flat spectrum sources are viewed pole-on or else have partially dissipated their envelopes (Calvet et al. 1994; Kenyon et al. 1993b).

We have found seven new Class I/flat spectrum YSOs in the cloud. GY 11 is an additional new flat spectrum source ($a = 0.1$) based on mid-IR photometry presented by CRBR. Interestingly, all of these Class I/flat spectrum sources are $K \geq 10$, and four of them are associated with radio continuum sources (see Table 2). *IRAS* was limited to the detection of $L \gtrsim 1\ L_\odot$ Class I YSOs due to extinction in the ρ Oph cloud

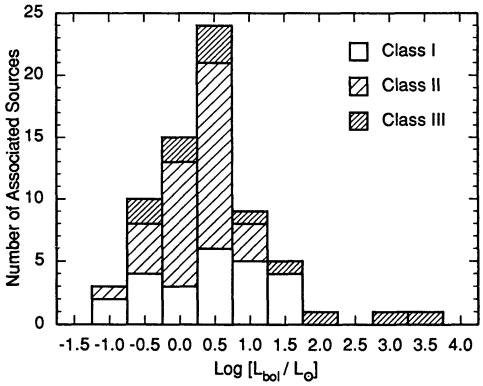

FIG. 4.—Luminosity function of the combined new L1688 sample and the previously studied population. Sources are grouped by SED classification within each luminosity bin.

core (WLY), so the nondetection of these sources in the WLY *IRAS* survey also strongly suggests that they are low-luminosity objects, $L \lesssim 1\ L_\odot$. Four radio continuum sources in our new sample were also found to be low-luminosity Class III sources (Tables 1 and 2). There are an additional 20 or more radio sources in the cloud that are either associated with a faint GY source or else have no $K < 13$ association (Leous et al. 1991). Therefore there may be a substantial population of low-luminosity YSOs in the cloud with radio continuum emission, but this will have to be verified with a more sensitive IR survey in the future.

Figure 4 shows that there are more intermediate-luminosity Class I than Class II YSOs in the combined sample, reinforcing the luminosity segregation of YSO classes first proposed by WLY. A total of nine Class I sources occupy the $L > 5.6\ L_\odot$ luminosity bins while only three Class II sources fall in those bins. Four of these Class I sources lie in the $18\ L_\odot < L < 56\ L_\odot$ bin, while no Class II source is this luminous. In contrast, only nine Class I sources occupy the $0.56\ L_\odot < L < 5.6\ L_\odot$ bins, while 25 Class II sources fall in these bins.

Despite incompleteness effects and uncertainties in luminosities and SED classifications, the luminosity segregation between Class I and II YSOs in Figure 4 appears to be a real effect. $L > 1\ L_\odot$ Class I YSOs can be detected throughout the cloud, but $L = 1\ L_\odot$ Class II YSOs are detected only if buried less than halfway into the $A_v \geq 50$ cloud core (WLY; see § 3.2.4). We estimate that only approximately 12% of the combined sample region has a mean $A_v > 25$, so this greater incompleteness of Class II YSOs should not be significant. In any case, greater incompleteness of Class II YSOs could not produce the observed luminosity segregation. The *IRAS* luminosities of these Class I and Class II sources are also subject to uncertainties due to source confusion from the relatively low spatial resolution of *IRAS* (45″) and the high density of ρ Oph sources. WLY find that many *IRAS*-detected YSOs have 12 μm fluxes that are about a factor of 2 larger than expected from ground-based 10–20 μm small aperture (~6″) photometry. Kenyon et al. (1990) and AM have argued that such discrepancies could mean that several YSOs may be often detected in a single *IRAS* beam, and this could enhance both the number and luminosity of Class I YSOs in the ρ Oph cloud. However, examination of the spatially complete near-IR survey of GY reveals no additional strong near-IR sources which could fall in the *IRAS* beams of detected Class I YSOs.

This luminosity segregation between Class I and Class II

© American Astronomical Society • Provided by the NASA Astrophysics Data System

1994ApJ...434..614G

YSOs can be interpreted in either or both of two ways. First, the higher luminosity Class I YSOs may be more massive and consequently intrinsically more luminous than Class II YSOs if star formation in the cloud is proceeding sequentially by mass. The warm $T \simeq 20$ K gas (Loren, Wootten, & Wilking 1990) and dust (Greene & Young 1989) temperatures observed in the dense cloud cores imply that higher mass stars may be forming now if the cloud was originally at lower temperatures, since the Jeans mass is proportional to $T^{1.5}$. Additionally, the detection of spatially extended mid-IR hydrocarbon emissions in the envelopes of the Class I/flat spectrum YSOs WL 16 and WL 22 (Hanner, Tokunaga, & Geballe 1992; Emerson 1994) strongly implies the presence of an ultraviolet (UV) radiation field emanating from these YSOs. A likely source of this radiation is the hot photospheres of intermediate- or high-mass stars, so there may be at least a few young massive Class I/flat spectrum YSOs forming in the cloud now. However, a number of high-mass main-sequence stars also exist in the cloud (e.g., see LW), so it is unclear if star formation is actually proceeding sequentially by mass. Second, if the Class I YSOs have similar masses to Class II sources, then the Class I YSOs have excess luminosity. This excess luminosity is likely the result of mass accretion occurring in the younger Class I YSOs, consistent with their interpretation as protostellar objects (ALS). Stahler, Shu, & Taam (1980) showed that a 1 $M_\odot$ YSO will reach a maximum luminosity of 66 $L_\odot$ during its accretion phase, declining to about 6 $L_\odot$ when it reaches the stellar birthline and starts its PMS (Class II) evolutionary phase (Stahler 1983; WLY).

4.3. *Comparisons with Taurus-Auriga*

The Taurus-Auriga clouds have a continuous distribution of Class I sources whose numbers increase with decreasing luminosity to below 1 $L_\odot$ (Kenyon et al. 1990, 1993a, 1994; Beichman, Boulanger, & Moshir 1992). The low extinction in the Taurus-Auriga clouds allowed *IRAS* to detect Class I sources completely down to $L = 0.1\ L_\odot$ (Beichman et al. 1992; Kenyon et al. 1994), 10 times fainter than the Class I *IRAS* detection limit through the ρ Oph cloud. The relatively abundant low-luminosity ($L \sim 0.5\ L_\odot$) Class I population in Taurus-Auriga is quite intriguing, since these sources must be extremely young ($\tau \sim 10^4$ yr) if they are accreting mass at the rate characteristic of the Taurus-Auriga clouds (Kenyon et al. 1990, 1993a; Beichman et al. 1992).

It is clear from the existing data that the $L > 1\ L_\odot$ Class I populations of the Ophiuchus and Taurus-Auriga clouds are considerably different. The distribution of Class I YSOs in Taurus-Auriga peaks at approximately 0.5 $L_\odot$ (Kenyon et al. 1994), but Figure 4 shows that most of the known Ophiuchus Class I YSOs have luminosities $1.8\ L_\odot < L < 56\ L_\odot$. The mean luminosity of $L > 1\ L_\odot$ Class I sources in the ρ Oph cloud is 11.6 $L_\odot$, while the mean luminosity of $L > 1\ L_\odot$ Class I YSOs in Taurus-Auriga is 5.2 $L_\odot$ (Kenyon et al. 1993a; Emerson et al. 1984). This factor of 2 Class I luminosity difference can be understood in terms of the different physical conditions in the two cloud regions. The higher temperature of dense gas in ρ Oph ($T \simeq 20$ K) compared to Taurus-Auriga ($T \simeq 10$ K; Myers & Benson 1983) implies that the ρ Oph accretion rate is 3 times higher than in Taurus-Auriga. The accretion rate is defined by Shu (1977) as $\dot{M} = a^3/G$, where $a = (kT/m)^{1/2}$ is the isothermal sound speed, 0.2 km s^{-1} in Taurus-Auriga and 0.28 km s^{-1} in ρ Oph. This simple derivation of sound speed does not consider turbulent or magnetic support of cloud gas, and we ignore these local effects in this general comparison of the two regions. Therefore the accretion luminosity, $L_{\rm acc} = GM\dot{M}/R = 72\ L_\odot\ (a/0.35\ {\rm km\ s^{-1}})^2 (M/M_\odot)$ (ALS), is twice as high in Ophiuchus ($47\ L_\odot\ M/M_\odot$) as in Taurus-Auriga ($24\ L_\odot\ M/M_\odot$). Class I sources of equal mass should be twice as luminous in Ophiuchus as in Taurus-Auriga since accretion is presumably the dominant luminosity source in the Class I YSO phase. Therefore the observed mean luminosity differences between $L > 1\ L_\odot$ Class I YSOs in Taurus-Auriga and the ρ Oph cloud can be explained almost entirely by accretion luminosity differences due to cloud conditions without invoking different mass functions.

However, it is important to note that the mass of such an average intermediate-luminosity Class I YSO in either cloud would be approximately 0.2 $M_\odot$ if the above accretion rates are adopted. This is considerably lower than the T Tauri masses found in either cloud (e.g., see Cohen & Kuhi 1979). Furthermore, the existence of a substantial low-luminosity ($L < 1\ L_\odot$) Class I population in Taurus-Auriga and at least several such sources in Ophiuchus suggests that even lower mass objects are present in both clouds if their luminosities are attributed totally to accretion. These low masses could be understood if there has been a recent burst of star formation in both clouds and the Class I sources are very young ($\tau < 10^4$ yr). However, this is a very small age compared to the accretion timescales $\tau_{\rm emb} > 10^5$ yr in both clouds (WLY; Kenyon et al. 1990, 1994). Perhaps the most likely explanation is that accretion is occurring in both clouds at lower rates than the characteristic $\dot{M} = a^3/G$, also suggested for Taurus-Auriga by Kenyon et al. (1993, 1994).

Chen et al. (1994) have recently acquired and assembled multiwavelength data and have determined that young embedded stars of similar age and bolometric temperature (Myers & Ladd 1993) exist in both the Ophiuchus and Taurus-Auriga clouds. The youngest sources in both clouds have similar bolometric temperatures, but the YSOs in ρ Oph are systematically more luminous. This further supports the argument that the Class I YSOs in Ophiuchus have higher accretion luminosities than those in Taurus-Auriga.

The relative numbers of Class I to Class II sources are factors of 2 smaller in the Taurus-Auriga and Chamaeleon I clouds than in the ρ Oph cloud (Kenyon et al. 1990; Prusti et al. 1992). This may be because star formation activity in the core of the ρ Oph cloud is recent, while the Taurus-Auriga clouds contain many regions of star formation that may not be coeval. The older regions would have fewer Class I sources, diluting the ratio of Class I to II sources when compared to the ρ Oph cloud (see Zinnecker et al. 1993). The YSOs in Chamaeleon I may also be older than those in the ρ Oph cloud, also resulting in relatively more Class II YSOs there.

4.4. *Duration of the Embedded Phase*

The additional data presented herein allows a reexamination of the lifetime of the Class I phase of YSO evolution. If star formation has proceeded at a uniform rate within the cloud and the Class I state is an evolutionary precursor to the Class II state, then the relative numbers of Class I and II sources should be proportional to the relative lifetimes of the two evolutionary phases. WLY estimated that these two phases have approximately equal lifetimes from the approximately equal numbers of Class I and Class II YSOs in the cloud down to 1 $L_\odot$ (after correcting for the *IRAS* selection bias against Class II sources). Figure 3 shows that the spectral indices computed for

© American Astronomical Society • Provided by the NASA Astrophysics Data System

1994ApJ...434..614G

objects in this survey are somewhat different from those of the previously studied population (mostly WLY *IRAS*-selected), so we now recompute the Class I lifetime using statistics of the combined sample. The combined sample includes 11 Class I, 22 Class II, and five flat spectrum sources with $L > 1\ L_\odot$. The number of Class II YSOs has been corrected for incompleteness to $L \sim 1\ L_\odot$ by doubling their number between 1 and 2 $L_\odot$. Sixteen YSOs are Class I or flat spectrum, and this constitutes 42% of the combined $L \geq 1\ L_\odot$ Class I, II, and flat spectrum population. If star formation has proceeded continuously in the cloud, then the embedded phase (Class I and flat spectrum) lifetime must be approximately 75% of the Class II lifetime. If the average Class II (T Tauri) lifetime is 4×10^5 yr from the birthline (WLY), then the typical class I lifetime is approximately 3×10^5 yr.

This procedure is the most direct way of calculating the embedded phase lifetime, but it contains biases that may artificially lengthen the calculated lifetime. First, Class III YSOs may actually be naked T Tauri stars in similar evolutionary phases as the Class II CTTSs. If this were true, then we would have to compare the number of Class I YSOs to the number of the entire YSO population (Class I + Class II + Class III) in order to estimate the embedded phase lifetime. The combined sample and recent *ROSAT* data (Casanova et al. 1994) show that there may be as many Class III as Class II YSOs in the cloud core. Second, the five flat spectrum sources may be a in a physical state that is a transition between the Class I and II YSO phases, so we must also consider counting them as Class II YSOs. Both of these effects lead us to regard our 3×10^5 estimate as the *maximum* likely lifetime of the embedded (Class I) phase in the ρ Oph cloud. We have calculated the *minimum* likely embedded phase lifetime to be 10^5 yr based on consideration of the biases discussed above. We conclude that the embedded phase lifetime of YSOs in the ρ Oph cloud is $(2 \pm 1) \times 10^5$ yr. Therefore a 1 $M_\odot$ YSO would accrete at the rate $\dot{M} = (3\text{–}10) \times 10^{-6}\ M_\odot\ \mathrm{yr}^{-1}$ over this lifetime, consistent with the $\dot{M} = 5 \times 10^{-6}\ M_\odot\ \mathrm{yr}^{-1}$ rate derived from cloud temperatures in § 4.3. Consequently, this embedded phase lifetime estimate appears to be approximately correct, and it also agrees with the Class I lifetime computed for the cloud by CRBR (1.5×10^5 yr). This new estimate of the embedded phase lifetime is consistent with the Kenyon et al. (1990) estimate of $(1\text{–}2) \times 10^5$ yr for Taurus-Auriga.

4.5. *Source Masses*

We have estimated masses of all Class II and III YSOs in the combined sample by using mass-luminosity relations derived from the DM PMS models. The 10^6 yr DM CM Alexander isochrone was chosen because this is representative T Tauri age in the cloud (see WLY). DM calculate that PMS masses between 0.1 $M_\odot$ and 2.5 $M_\odot$ change by less than a factor of 2 between the ages of 5×10^5 yr and 3×10^6 yr. The good agreement between the L_{bol} versus $F(J_0)$ curve of the DM-McCaughrean models and the empirical fit suggests that these models do accurately represent most Classs II YSOs (see Fig. 2 and § 3.2.3), so masses derived from them should be good estimates of real Class II stellar masses. The DM models were calculated for stars with no circumstellar material, so they should also provide good mass estimates for Class III sources. We have assumed that the Class III YSOs in the cloud are the same age as Class II ones, resulting in slightly greater uncertainties in their mass estimates. The distribution of masses for all Class II and III sources in the combined sample with $L < 10\ L_\odot$ is shown in Figure 5. Mass is binned by factors of 3.2 in Figure 5, so we expect that the form of this mass function adequately represents the Class II and III cloud population if these YSOs have ages between 5×10^5 and 3×10^6 yr.

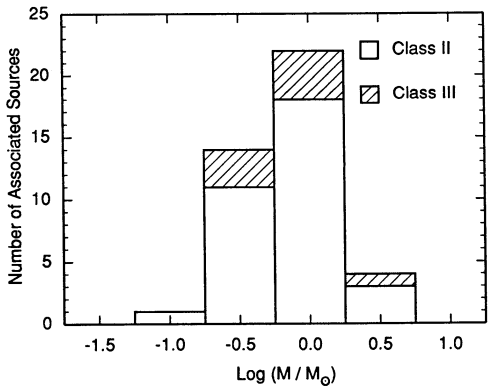

FIG. 5.—Mass function of Class II and III YSOs associated with the ρ Oph cloud. Masses were calculated from the DM 10^6 yr PMS model isochrone. The Class II masses are incomplete at $M \lesssim 0.5\ M_\odot$, and the Class III mass function is incomplete at all masses.

Most Class II and III YSOs have masses between 0.2 and 2.0 $M_\odot$ when computed in this fashion. The average Class II stellar mass is 1.0 $M_\odot$, and the most massive one is S2, $M \simeq 2.5\ M_\odot$ (see Fig. 5). These masses are similar to those of PMS stars in the Taurus-Auriga clouds (e.g., see Cohen & Kuhi 1979). The Class II mass function in Figure 5 appears to be increasing toward lower masses until incompleteness effects become significant ($M \lesssim 0.5\ M_\odot$). The Class III population in Figure 5 is incomplete at all masses due to the small numbers of Class III sources associated with the cloud via corroborating data at other wavelengths. This is the most accurate mass estimation technique possible using the data of the combined YSO sample. This technique offers an attractive alternative to mass determination via spectroscopic classification, since it can be applied to optically invisible objects, and it only requires the acquisition of photometric data.

5. SUMMARY

We have completed a new IR study of YSOs in the ρ Oph cloud. The sample was assembled from all $K < 10$ mag sources detected by GY near the cloud core, fainter near-IR sources that are red, and fainter sources with radio continuum emission. These data have been combined with previous surveys in order to characterize star formation in the cloud as well as possible. We find the following major results:

1. Our study has revealed 10 new Class II sources. As expected, the cloud has a larger population of low-luminosity Class II YSOs than found by *IRAS*. All $K < 10$ sources have Class II or III SEDs, while sources with radio continuum emission have Class I or III SEDs. We have found seven new low-luminosity ($L \lesssim 1\ L_\odot$) Class I and flat spectrum sources in the cloud. These YSOs are faint in the near-IR ($K \geq 10$), and four of them are also associated with radio continuum emission. Radio continuum surveys suggest that these sources may be part of a larger population of low-luminosity YSOs, but this must be verified with new sensitive mid-IR data.

2. We have found strong empirical linear correlations between L_{bol} and the dereddened J- or K-band flux for a large sample of low-mass Class II YSOs in nearby clouds. Such

© American Astronomical Society • Provided by the NASA Astrophysics Data System

1994ApJ...434..614G

correlations are expected given the small range of temperatures and similarity of SEDs of Class II YSOs. The L_{bol} versus $F(J_0)$ relation is similar to a theoretical one predicted by the DM-McCaughrean PMS stellar models, strongly suggesting that most Class II objects are indeed PMS stars with little fractional accretion luminosity. These empirical relations were used to estimate bolometric luminosities for our new sample of ρ Oph YSOs. Unlike calorimetric luminosity estimates, the effects of interstellar absorption are removed from these empirically derived estimates by dereddening near-IR data. These estimates are within a factor of 2 of true bolometric luminosities.

3. Most of the intermediate-luminosity ($5.6\ L_\odot < L < 56\ L_\odot$) YSOs in the cloud are Class I sources, while Class II YSOs significantly outnumber Class I sources in the $0.56\ L_\odot < L < 5.6\ L_\odot$ range. This luminosity segregation could be the result of accretion luminosity in Class I YSOs. The relative numbers of sources with different SED classifications suggest that the lifetime of the embedded phase of YSO evolution in the ρ Oph cloud is approximately $(2 \pm 1) \times 10^5$ yr after correcting for selection effects and biases.

4. Comparisons with Taurus-Auriga reveal that the higher luminosities of Class I YSOs in ρ Oph may be accounted for by a higher mass accretion rate in the ρ Oph cloud. This is consistent with the different kinetic gas temperatures found in dense cores in the two clouds. The embedded phase lifetime is also found to be similar in the two clouds.

5. We have derived masses for Class II and III YSOs in the combined sample by using the PMS stellar models of DM. These models indicate that the average Class II stellar mass is 1.0 $M_\odot$, while we incompletely detect Class II YSOs with masses below about 0.5 $M_\odot$. This technique offers an attractive alternative to mass determination from spectroscopic classifiction.

We thank G. Rieke and M. Meyer for assisting with observations and data reduction. We also thank S. Gordon, K. Strom, and M. McCaughrean for providing data and results in advance of publication. T. P. G. gratefully acknowledges the IRTF and the National Research Council for supporting this work, and we thank all MMT, IRTF, and CTIO telescope operators for their assistance. IRAF is distributed by the National Optical Astronomy Observatories, operated by the Association of Universities for Research in Astronomy, Inc., under contract to the National Science Foundation.

REFERENCES

Adams, F. C., Lada, C. J., & Shu, F. H. 1987, ApJ, 213, 788 (ALS)
Alexander, D. R., Augason, G. C., & Johnson, H. R. 1989, ApJ, 345, 1014
André, P., & Montmerle, T. 1994, ApJ, 420, 837 (AM)
André, P., Montmerle, T., & Feigelson, E. D., 1987, AJ, 93, 1182 (AMF)
Barsony, M., Burton, M. G., Russell, A. P. G., Carlstrom, J. E., & Garden, R. 1989, ApJ, 346, L93
Beichman, C. A., Boulanger, F. & Moshir, M. 1992, ApJ, 386, 248
Bouvier, J., & Apenzeller, I. 1992, A&AS, 92, 481
Calvet, N., Hartmann, L., Kenyon, S., & Whitney, B. A. 1994, preprint
Canuto, V. M., & Mazzitelli, I. 1992, ApJ, 389, 724
Casanova, S., Montmerle, T., Feigelson, E. D., & André, P. 1994, ApJ, in press
Chen, H., Myers, P. C., Ladd, E. F., & Wood, D. O. S. 1994, in preparation
Chini, R. 1981, A&A, 99, 346
Cohen, M., & Kuhi, L. V. 1979, ApJS, 41, 743
Comeron, F., Rieke, G. H., Burrows, A., & Rieke, M. J. 1993, ApJ, 416, 185 (CRBR)
D'Antona, F., & Mazzitelli, I. 1994, ApJS, 90, 467 (DM)
Dolidze, M. V., & Arakeylan, M. A. 1959, Soviet Astron, 3, 434
Elias, J. H. 1978, ApJ, 224, 453
Emerson, J. P. 1994, in preparation
Emerson, J. P., et al. 1984, ApJ, 278, L49
Gauvin, L. S., & Strom, K. M. 1992, ApJ, 385, 217
Gordon, S., & Strom, K. M. 1990, private communication
Grasdalen, G. L., Strom, K. M., & Strom, S. E. 1973, ApJ, 184, L53 (GSS)
Greene, T. P. 1994, in preparation
Greene, T. P., & Young, E. T. 1989, ApJ, 339, 258
———. 1992, ApJ, 395, 516 (GY)
Hanner, M. S., Tokunaga, A. T., & Geballe, T. 1992, ApJ, 395, L111
Kenyon, S. J., Calvet, N., & Hartmann, L. 1993a, ApJ, 414, 676
Kenyon, S. J., Gomez, M., Marzke, R. O., & Hartmann, L. 1994, AJ, submitted
Kenyon, S. J., Hartmann, L. W., Strom, K. M., & Strom, S. E. 1990, AJ, 99, 869
Kenyon, S. J., Whitney, B. A., Gomez, M., & Hartmann, L. 1993b, ApJ, 414, 773
Laçon, A., & Rocca-Volmerange, B. 1992, A&AS, 96, 593
Lada, C. J. 1987, in Star Forming Regions, ed. M. Peimbert & J. Jugaku (Dordrecht: Reidel), 1
Lada, C. J., & Wilking, B. A. 1984, ApJ, 287, 610 (LW)
Leous, J. A., Feigelson, E. D., André, P., & Montmerle, T. 1991, ApJ, 379, 683 (LFAM)
Loren, R. B., Wootten, A., & Wilking, B. A. 1990, ApJ, 365, 269
Lynden-Bell, D., & Pringle, J. E. 1974, MNRAS, 168, 603
McCaughren, M. J. 1993, private communication
Montmerle, T., Koch-Miramond, L., Falgarone, E., & Grindlay, J. E. 1983, ApJ, 269, 182
Myers, P. M., & Benson, P. J. 1983, ApJ, 266, 309
Myers, P. M., Fuller, G. A., Mathieu, R. D., Beichman, C. A., Benson, P. J., & Schild, R. E. 1987, ApJ,319, 340
Myers, P. M., & Ladd, E. 1993, ApJ, 413, L47
Prusti, T., Whittet, D. C. B., & Wesselius, P. R. 1992, MNRAS, 254, 361
Rieke, G. H., & Lebofsky, M. J. 1985, ApJ, 288, 618 (RL)
Rogers, F. J., & Iglesias, C. A. 1992, ApJS, 79, 507
Rucinski, S. M. 1985, AJ, 90, 2321
Rydgren, A. E., Schmelz, J. T., Zak, D. S., & Vrba, F. J.1984, Publ. US Naval Obs., 25, pt. 1
Rydgren, A. E., Strom, S. E., & Strom, K. M. 1976, ApJS, 30, 307
Stahler, S. W. 1983, ApJ, 274, 822
Stahler, S. W., Shu, F. H., & Taam, R. E. 1980, ApJ, 241, 637
Strom, K. M., Strom, S. E., & Merrill, K. M. 1993, ApJ, 412, 233 (SSM)
Struve, O., & Rudkjøbing, M. 1949, ApJ, 109, 92
Shu, F. H. 1977, ApJ, 214, 488
Vrba, F. J., Strom, S. E., & Strom, K. M. 1976, AJ, 81, 958
Vrba, F. J., Strom, K. M., Strom, S. E., & Grasdalen, G. L. 1975, ApJ, 197, 77 (VSSG)
Walter, F. M., Vrba, F. J., Mathieu, R. D., Brown, A., & Meyers, P. C. 1994, AJ, in press
Ward-Thompson, D. 1993, MNRAS, 265, 493
Wilking, B. A., Greene, T. P., Lada, C. J., Meyer, M. R., & Young, E. T. 1992, ApJ, 397, 520
Wilking, B. A., & Lada, C. J. 1983, ApJ, 274, 698 (WL)
Wilking, B. A., Lada, C. J., & Young, E. T. 1989, ApJ, 340, 823 (WLY)
Wilking, B. A., Schwartz, R. D., & Blackwell, J. H. 1987, AJ, 94, 106 (WSB)
Young, E. T., Lada, C. J., & Wilking, B. A. 1986, ApJ, 304, L45
Young, E. T., Neugebauer, G., Kopan, E. L., Benson, R. D., Conrow, T. P., Rice, W. L., & Gregorich, D. T. 1985, A Users Guide to the *IRAS* Pointed Observation Products, IPAC preprint PRE-008N
Zinnecker, H., McCaughrean, M. J., & Wilking, B. A. 1993, in Protostars and Planets III, ed. G. Levy & J. Lunine (Tucson: Univ. Arizona Press), 429

© American Astronomical Society • Provided by the NASA Astrophysics Data System